Supplementary information

Facile polymer-assisted synthesis of $LiNi_{0.5}Mn_{1.5}O_4$ with hierarchical micro-nano structure and high rate capability

Xiaolong Zhang, Fangyi Cheng, Kai Zhang, Yanliang Liang, Siqi Yang, Jing Liang, and Jun Chen*

Key Laboratory of Advanced Energy Materials Chemistry (Ministry of Education), College of Chemistry, Nankai University, Tianjin, 300071, People's Republic of China. E-mail: chenabc@nankai.edu.cn; Tel/Fax: +86-22-23506808.

This file contains Figs. S1–S3.

To gain insight into the growth process of the product, thermogravimetric analysis was performed on LNMO-PEG4000 precursor in air flow with a heating rate of 10 °C min^{-1}. Typical Mass/DTG (Differential TG) curves are shown in Fig. S1. The weight loss of the precursor mainly occurred between 200 and 360 °C with DTG peaks at 212, 263, 307, and 354 °C. Three parallel samples of LNMO-PEG4000 precursor were heated to 250 °C (during the main weight loss process), 360 °C (immediately after the main weight loss process), and 800 °C (the calcination temperature) respectively. Phase transfer during the heating process was characterized by XRD. The results are shown in Fig. S2a-d. Five main patterns (PEG, $H_2C_2O_4$, $MnC_2O_4{\cdot}2H_2O$, $NiC_2O_4{\cdot}2H_2O$, and $Li_2C_2O_4$) can be identified in the XRD graph of the pristine precursor (Fig. S2a). This is reasonable since the $H_2C_2O_4$ was much excessive, and the original acetate should react with oxalate acid to form the oxalate. When heated to 250 °C (Fig. S2b), the PEG peaks at $2\theta = 19°$ and 22° were dramatically weakened, indicating that the PEG combustion mainly proceeded before 250 °C. Three patterns of oxalates ($MnC_2O_4{\cdot}2H_2O$, $NiC_2O_4{\cdot}2H_2O$, and $Li_2C_2O_4$) were detected at this stage. When the temperature was elevated to 360 °C (Fig. S2c), characteristic peaks of $Li_2C_2O_4$ and a strong diffraction patterns of spinel phase $LiMn_2O_4$ were identified. As $Li_2C_2O_4$ was not completely decomposed yet, extra Mn_3O_4 and $Li_xNi_{1-x}O$ also exsist in the mixture. For the sample being calcined at 800 °C (Fig. S2d), a strong spinel $LiNi_{0.5}Mn_{1.5}O_4$ phase was finally detected.

JCPDS card numbers of all the labelled phases in Fig. S2a-d were listed below:

PEG	49-2109
$MnC_2O_4{\cdot}2H_2O$	25-0544
$NiC_2O_4{\cdot}2H_2O$	25-0581
$H_2C_2O_4$	20-1817
$Li_2C_2O_4$	24-646
$LiMn_2O_4$	35-0782
Mn_3O_4	24-0734
$Li_xNi_{1-x}O$	44-1159
$LiNi_{0.5}Mn_{1.5}O_4$	80-2162.

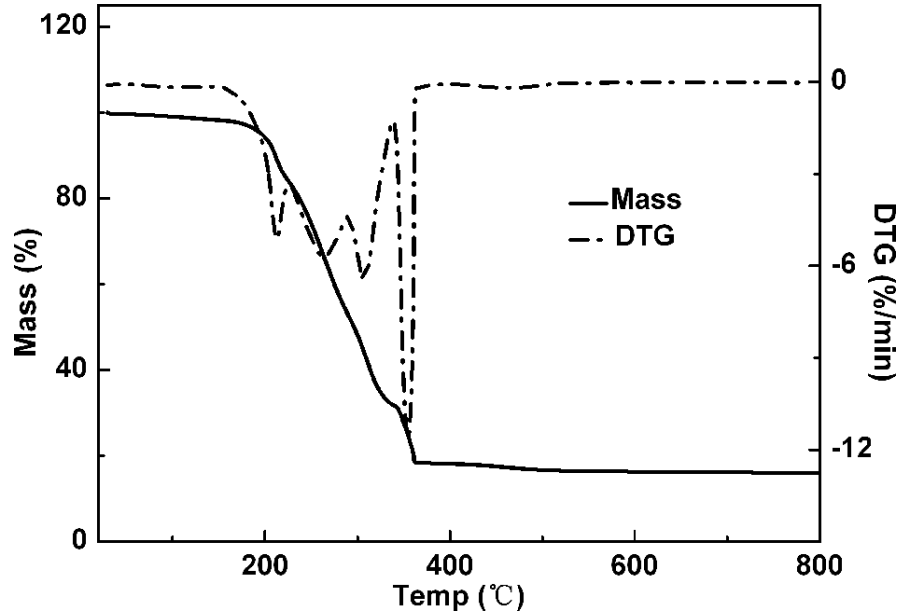

Fig. S1 TG/DTG curves of LNMO-PEG4000 precursor.

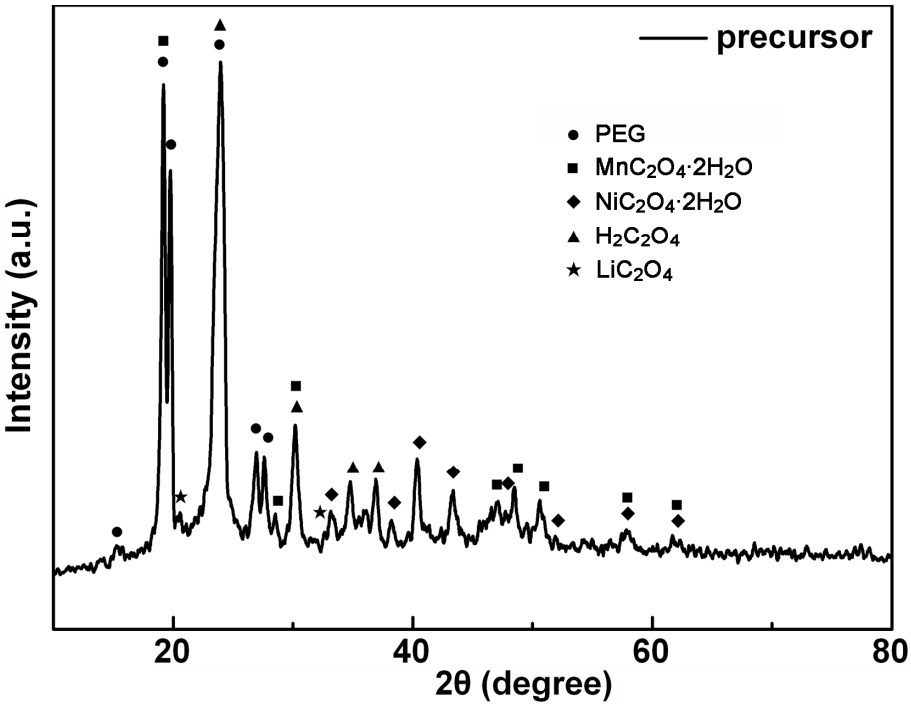

Fig. S2a XRD pattern of the LNMO-PEG4000 pristine precursor.

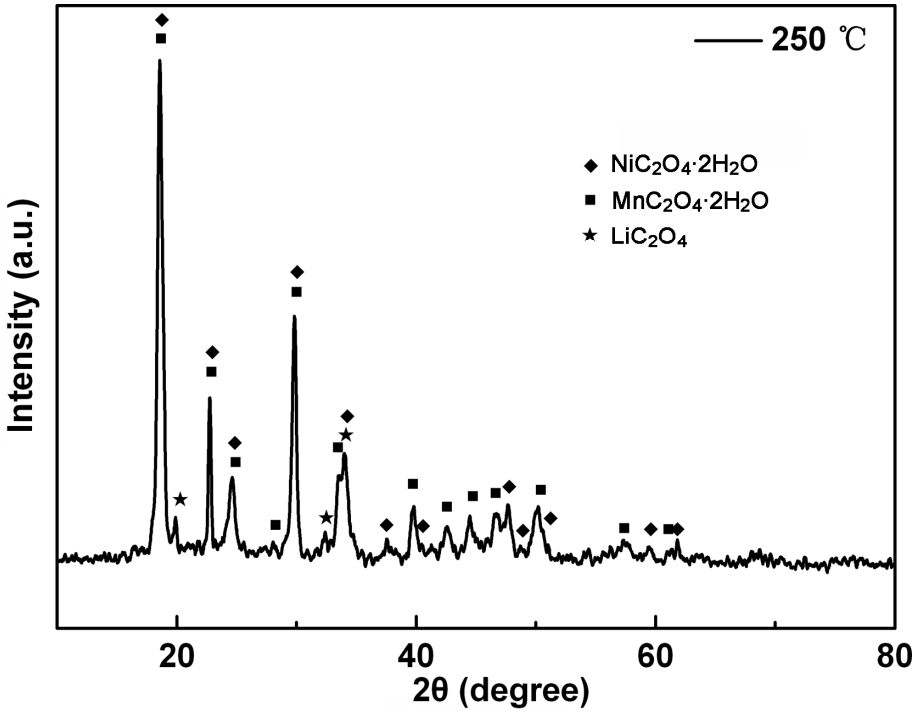

Fig. S2b XRD pattern of the LNMO-PEG4000 precursor heated to 250 °C.

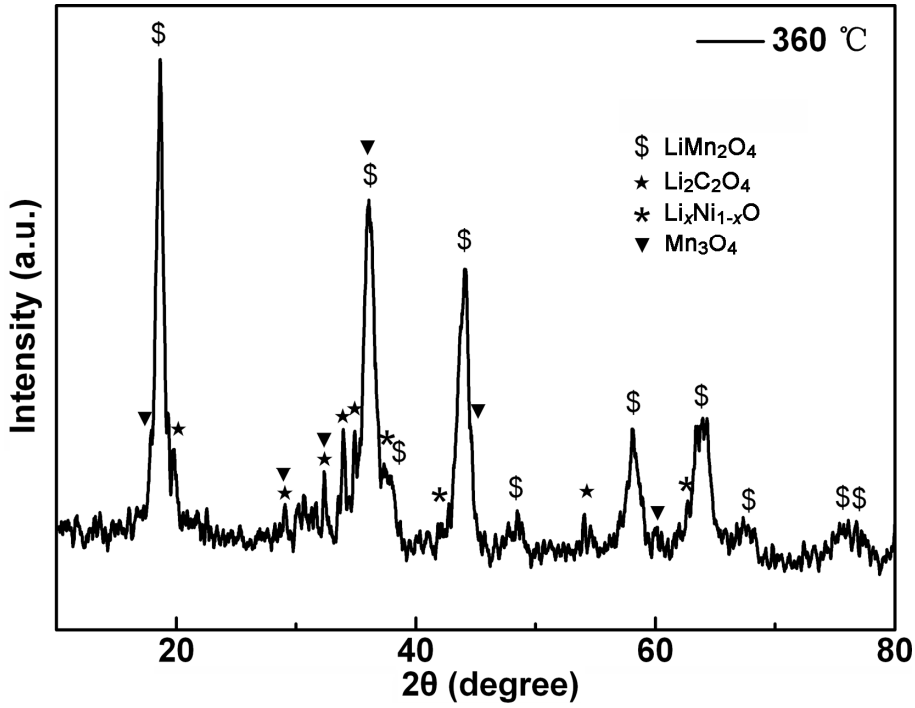

Fig. S2c XRD pattern of the LNMO-PEG4000 precursor heated to 360 °C.

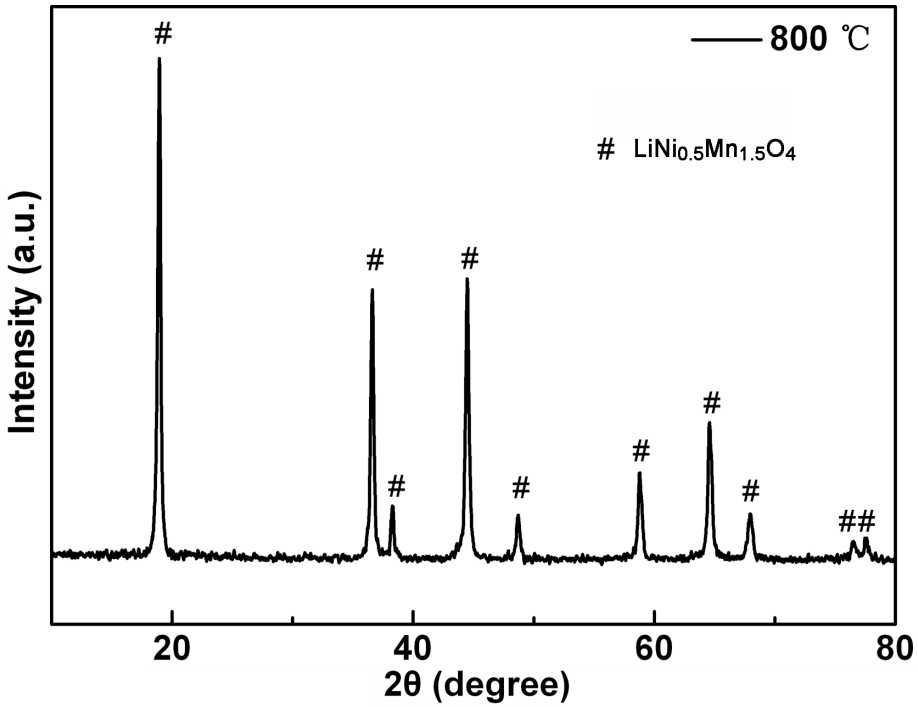

Fig. S2d XRD pattern of the LNMO-PEG4000 precursor heated to 800 °C.

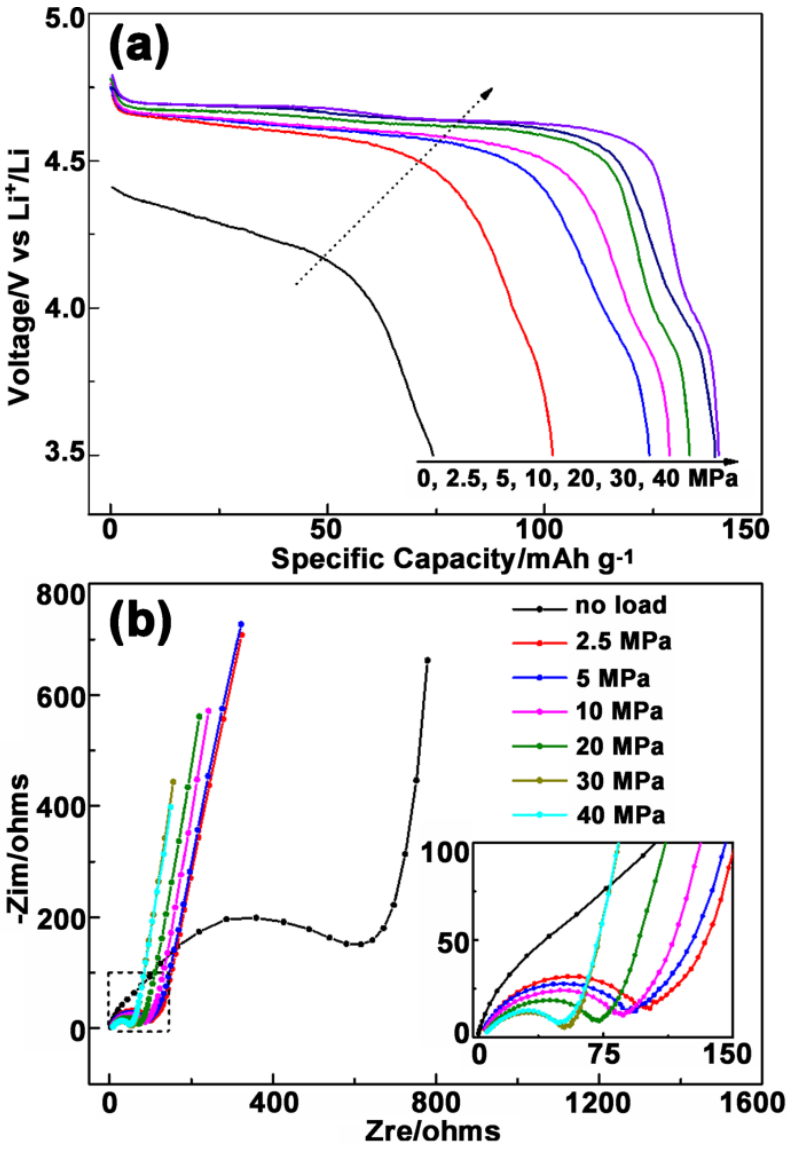

Fig. S3 (a) Discharge curves (1C rate) and (b) Electrochemical impedance spectra of the electrodes fabricated with different load pressures. The dashed rectangle area in (b) is enlarged in the inset.

Different load pressures were directly applied to the dried paste on aluminium current collector. Fig. S3a shows the 1C discharge curves of the electrodes fabricated with different load pressure of 0, 2.5, 5, 10, 20, 30, and 40 MPa. The discharge capacity and plateau voltage increases with load pressure. Electrochemical impedance spectra of different electrodes were collected after charge–discharge at 1C rate for 5 cycles (Fig. S3b). All the spectra contain a semicircle in the high/medium frequency regions and a tail in the low frequency zone. The radius of the semicircle dramatically decreased when external pressure was applied. From the results of galvanostatic

discharge and EIS, it is reasonable to ascribe the much improved electrochemical performance of the electrode treated with high external pressure to the effectively diminished contact impedance between the composite paste (active materials, carbon, PVDF) and the current collector and the condensed intersection within the paste composite.[1]

Reference

1. M. Gaberscek, J. Moskon, B. Erjavec, R. Dominko and J. Jamnik, *Electrochem. Solid-State Lett.*, 2008, **11**, A170-A174.